Efimov States of Strongly Interacting Photons

M. J. Gullans,[1,2,*] S. Diehl,[3] S. T. Rittenhouse,[4] B. P. Ruzic,[1] J. P. D'Incao,[5,6] P. Julienne,[1] A. V. Gorshkov,[1,2,†] and J. M. Taylor[1,2,7,‡]

[1]*Joint Quantum Institute, NIST and University of Maryland, College Park, Maryland 20742, USA*
[2]*Joint Center for Quantum Information and Computer Science, NIST and University of Maryland, College Park, Maryland 20742, USA*
[3]*Institut für Theoretische Physik, Universität zu Köln, D-50937 Cologne, Germany*
[4]*Department of Physics, The United States Naval Academy, Annapolis, Maryland 21402, USA*
[5]*JILA, University of Colorado and NIST, Boulder, Colorado 80309, USA*
[6]*Department of Physics, University of Colorado, Boulder, Colorado 80309, USA*
[7]*Research Center for Advanced Science and Technology (RCAST), The University of Tokyo, Meguro-ku, Tokyo, 153-8904, Japan*

(Received 20 August 2017; published 4 December 2017)

We demonstrate the emergence of universal Efimov physics for interacting photons in cold gases of Rydberg atoms. We consider the behavior of three photons injected into the gas in their propagating frame, where a paraxial approximation allows us to consider them as massive particles. In contrast to atoms and nuclei, the photons have a large anisotropy between their longitudinal mass, arising from dispersion, and their transverse mass, arising from diffraction. Nevertheless, we show that, in suitably rescaled coordinates, the effective interactions become dominated by s-wave scattering near threshold and, as a result, give rise to an Efimov effect near unitarity. We show that the three-body loss of these Efimov trimers can be strongly suppressed and determine conditions under which these states are observable in current experiments. These effects can be naturally extended to probe few-body universality beyond three bodies, as well as the role of Efimov physics in the nonequilibrium, many-body regime.

DOI: 10.1103/PhysRevLett.119.233601

The problem of classifying the universal properties of few-body systems near unitarity, i.e., a divergence in the two-body scattering length a, was first undertaken for the three-body problem by Vitaly Efimov in 1970, who discovered an infinite series of three-body bound states obeying a geometrical scaling relation [1]. This discovery served as an important guide to theoretical work in few-body physics in subsequent years [2], but the observation of such Efimov trimers in nature remained elusive until pioneering experiments on cold atomic gases reported direct signatures of these states in atomic loss spectroscopy 3]]. That success reinvigorated work on the classification problem alluded to above, including in systems other than cold atoms [4,5]. As a result, recent years have seen the elucidation of many universal properties of N-body systems for $N \geq 3$ [6–13], including the many-body, short-time dynamics of Efimov trimers in a unitary Bose gas [14]. Despite this progress, Efimov states, as well as larger bound state clusters, are typically associated with large inelastic losses in cold atom systems due to strong three-body recombination. These losses generally preclude the study of many-body physics of Efimov trimers such as the formation of a Bose-Einstein condensate of trimers [15], and limit efforts to study universal bound states for large N.

Recently, it has become possible to achieve strong interactions between single photons by dressing light with strongly interacting Rydberg atoms to form Rydberg polaritons [16,17]. The resulting photon-photon interactions have been used to study a diverse array of quantum nonlinear optical effects including: single-photon blockade and transistors [18–22], two-photon phase gates [23–26], and the formation of one dimensional few-photon bound states [27–33]. Combining these strong interactions with the high degree of available control over the optical and atomic degrees of freedom makes these systems a promising platform for exploring nonequilibrium quantum many-body physics and realizing quantum simulation [34–44].

In this Letter, we show how such systems of interacting photons can lead to the formation of Efimov states of light. We extend previous work on bound states of photons in Rydberg polariton systems by accounting for the three-dimensional (3D) nature of the photons. For attractive interactions, these considerations lead to the possibility of forming 3D bound states, of which the Efimov states are the first class of three-body bound states that emerge as the strength of the interactions is increased from zero.

Crucial to the realization of Efimov states in this system is their low-energy, long-wavelength nature, which leads to their emergence independent of many of the microscopic details of Rydberg polaritons. We use this property to show that the three-body losses of these Efimov states can be strongly suppressed, allowing for the formation of long-lived Efimov trimers. We analytically demonstrate that this class of Efimov states have anisotropic spatial wave functions due to the anisotropic effective mass of the polaritons. To prepare these states, we take advantage of the fact that they propagate in the medium as the three-body limit of an optical soliton. This property allows them to be

distinguished from nonbound states in the system, which will dephase due to dispersive and diffractive effects [27,32]. Finally, we consider the conditions under which these states can be directly observed in current experiments.

The basic configuration for realizing interacting photons via atomic Rydberg states is shown in Fig. 1(a). The Rydberg atoms are dressed with a quantum field of light using electromagnetically induced transparency (EIT). Rydberg-Rydberg interactions lead to the Rydberg blockade effect [45], whereby a single atom (polariton) in the state $|s\rangle$ shifts the s state of nearby atoms out of resonance, leading to a strong optical nonlinearity. To describe the light transmission of this system, we introduce a bosonic field $\psi(\boldsymbol{r})$ associated with the Rydberg dark-state polaritons. The bare interaction between the Rydberg atoms is given by the van der Waals interaction $V(\boldsymbol{r}) = -C_6/r^6$; however, the effective interactions between polaritons take the form [see Fig. 1(b)] [28]

$$U(\boldsymbol{r}) = \frac{\alpha V(\boldsymbol{r})}{1 - \bar{\chi} V(\boldsymbol{r})}, \tag{1}$$

where $\bar{\chi}$ and α are a function of the control parameters and atomic decay rates [46]. Here, we consider the case $\bar{\chi}, C_6 > 0$ with a large detuning Δ from the intermediate state so that $U(\boldsymbol{r})$ is attractive, nonsingular, and conservative. $U(\boldsymbol{r})$ has a long range van der Waals tail, but saturates to a constant value for $r \ll r_b$, where the blockade radius is defined as $r_b = |\bar{\chi} C_6|^{1/6}$. Because of their low-energy, the Efimov states will have a spatial extent much larger than r_b [see inset to Fig. 1(b)]. We take advantage of the long-wavelength nature of these states to describe their propagation using the effective second-quantized Hamiltonian density

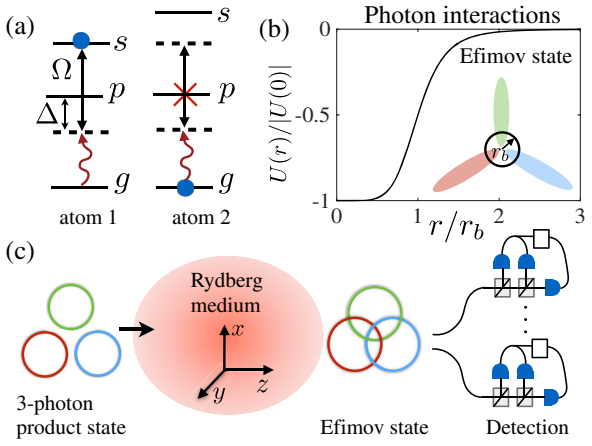

FIG. 1. (a) Schematic of EIT and the Rydberg blockade effect. (b) Effective interaction potential for the Rydberg polaritons. (inset) The Efimov states have a large spatial extent compared to the microscopic range of the potential, leading to many simplifications. (c) The Efimov states emerge in transmission because they are immune to dispersion and diffraction inside the medium. Spatially resolving multimode, three-photon coincidence measurements allow for detailed characterization of these states [32,53].

$$\mathcal{H} = \psi^\dagger(\boldsymbol{r})\left(-i\hbar v_g \partial_z - \frac{\hbar^2 \partial_z^2}{2m_z} - \frac{\hbar^2 \partial_\perp^2}{2m_\perp}\right)\psi(\boldsymbol{r}) + \int d^3 r' \psi^\dagger(\boldsymbol{r})\psi^\dagger(\boldsymbol{r}')U(\boldsymbol{r}-\boldsymbol{r}')\psi(\boldsymbol{r}')\psi(\boldsymbol{r}), \tag{2}$$

where v_g is the EIT group velocity, m_z is the longitudinal mass arising from dispersive effects, $m_\perp$ is the transverse mass arising from diffraction in the paraxial wave approximation, and $\partial_\perp^2 = \partial_x^2 + \partial_y^2$. The lowest order correction to this effective Hamiltonian is a short-range, three-body force [30–33]; however, such forces typically play a minor role in Efimov physics so we neglect them here [50–52].

After transforming into a comoving frame, apart from the anisotropic mass, the effective model has a standard form studied in few-body atomic and nuclear systems. Furthermore, near threshold, we find that the anisotropy in the mass can be accounted for by a simple rescaling of the coordinates and the scattering becomes isotropic in the absence of higher partial wave resonances. This implies that the universal few-body hierarchy, beginning with the Efimov effect, will arise near unitarity for such 3D Rydberg polaritons.

The preparation and detection scheme for the Efimov states is illustrated in Fig. 1(c). The entrance into the medium acts as a quantum quench [27,30], generating a finite overlap with the Efimov states. Once they are formed inside the medium, the bound states propagate without distortion, while the scattering states dephase with each other. As a result, for a sufficiently long medium in the absence of losses, the output will be dominated by the Efimov states. This effect has been used previously in 1D Rydberg polariton experiments to directly observe the formation of two and three-body bound states [27,32]. When there is more than one bound state in the medium, these states are distinguishable by their spatial structure or propagation phase through the medium. To directly probe these states, one can use time-resolved, three-photon coincidence measurements to access their longitudinal spatial structure, while multimode spatial resolution can probe their transverse structure [32,53].

Few-body scattering with anisotropic mass.—To understand the origin of the noninteracting part of Eq. (2), we consider the Hamiltonian for a single polariton with the total wave vector $k = \sqrt{(k_0 + q_z)^2 + q_\perp^2}$ ($\hbar = 1$)

$$H = \begin{pmatrix} ck - ck_0 & g & 0 \\ g & \Delta & \Omega \\ 0 & \Omega & 0 \end{pmatrix}, \tag{3}$$

where $\boldsymbol{q}$ is the momentum relative to $k_0\hat{z}$, $g = \mu_{\rm at}\sqrt{ck_0 n/\hbar\epsilon_0}$ is the single-photon Rabi frequency of the probe, ϵ_0 is the dielectric constant, n is the atomic density, $\mu_{\rm at}$ is the atomic dipole moment, Ω is the control field Rabi frequency, and Δ is the detuning between the control field and $|p\rangle$ to $|s\rangle$ transition frequency [see Fig. 1(a)]. We include the decay from the intermediate state by adding an imaginary

component to $\Delta \to \Delta - i\gamma$, where γ is the half-width of the p state. For every $\boldsymbol{q}$, H has three eigenvalues $\epsilon_\mu(\boldsymbol{q})$, which can be used to find the group velocity and effective mass of the polaritons

$$v_g = \left.\frac{d\epsilon_{\mu^*}}{dq_z}\right|_{\boldsymbol{q}^*} = c\frac{[\Omega^2+\omega(\Delta-\omega)]^2}{g^2(\Omega^2+\omega^2)}, \tag{4}$$

$$\frac{1}{m_z} = \left.\frac{d^2\epsilon_{\mu^*}}{dq_z^2}\right|_{\boldsymbol{q}^*} = \frac{2v_g^2}{\Omega^2+\omega^2}\frac{\Omega^2(\Delta-3\omega)-\omega^3}{\Omega^2+\omega(\Delta-\omega)}, \tag{5}$$

$$\frac{1}{m_\perp} = \left.\frac{d^2\epsilon_{\mu^*}}{dq_\perp^2}\right|_{\boldsymbol{q}^*} = \frac{v_g}{k_0}, \tag{6}$$

where $\epsilon_{\mu^*}(\boldsymbol{q}^*) = \omega$ is only satisfied for one choice of q^* and $\mu^* \in \{U, D, L\}$ [see Fig. 2(a)], and we take $\boldsymbol{q}_\perp^* = 0$. Here, we have neglected higher order corrections in Ω/g. From these expressions, we see that, on EIT resonance ($\omega = 0$), the mass ratio $m_z/m_\perp = g^2/2c\Delta k_0 = (3\pi\gamma/\Delta)nk_0^{-3}$.

More generally, the mass ratio can be independently tuned by taking advantage of the unconventional dispersion relation for the dark-state polaritons. This is illustrated in Fig. 2(a), which shows that the inverse longitudinal mass goes through a sign change for incoming probe frequencies away from the EIT resonance. From Eq. (4), we see that the inflection point occurs near $\omega = (\Omega^2\Delta)^{1/3}$. Operating near this inflection point allows one to equalize the mass ratio; however, it does not remove the effect of inelastic losses.

We define the average mass $m^{-1} = (m_z^{-1} + m_\perp^{-1})/2$ and parametrize the mass ratio as $\tan^2(\beta) = m_z/m_\perp$. The condition for neglecting the inelastic losses, which applies to both the EIT resonance and the inflection point in the limit $\Delta \gg \gamma, |\omega|$, is given by

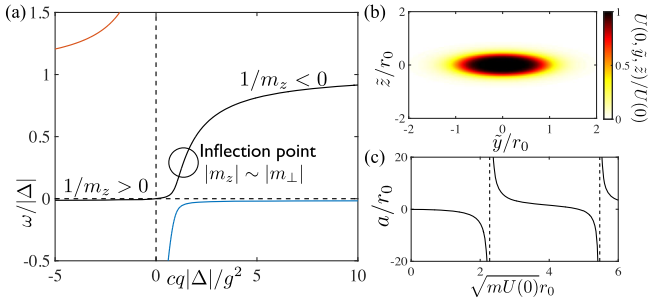

FIG. 2. (a) Dispersion relation near EIT resonance and inflection point for three polariton branches U (red), D (black), and L (blue). We took $\Omega/2\pi = 5$ MHz, $\Delta = 40$ MHz, and $g/2\pi = 100$ MHz. Here, g was taken to be smaller than its value in typical experiments to aid visibility. (b) Shape of potential in rescaled coordinates. (c) Scattering length as a function of the depth of the potential for $m_\perp/m_z = 10$. The first resonance occurs near $\sqrt{mU(0)}r_0 = 2.27$.

$$\frac{\mathrm{Re}(m^{-1})}{\mathrm{Im}(m^{-1})} \approx \frac{3\pi}{2\beta^2}\frac{n}{k_0^3} \gg 1. \tag{7}$$

For example, for atomic densities near 10^{13} cm^{-3}, β should be less than 0.1. It is also worth noting that the regime where $\beta \approx 1$ and Eq. (7) predicts small inelastic losses precisely coincides with the regime of Dicke super-radiance $n/k_0^3 \gtrsim 1$ [54]. In this regime, our assumption of independent decay channels for the atomic radiation would have to be revisited.

To understand the role of such a large anisotropy in the mass on the few-body scattering problem, we first consider the two-body problem with an anisotropic mass. The Schrödinger equation for two particles in the center of mass frame takes the form

$$-\frac{1}{m}\tilde{\nabla}^2\psi + U(\tilde{\boldsymbol{r}})\psi = E\psi, \tag{8}$$

where E is the energy and we have transformed to rescaled coordinates $\tilde{z} = z/\sqrt{2}\cos\beta$ and $(\tilde{x}, \tilde{y}) = (x, y)/\sqrt{2}\sin\beta$ such that the kinetic energy term becomes isotropic and the interactions become anisotropic [see Fig. 2(b)]. The characteristic length scale of the potential in the rescaled coordinates is given by $r_0 = r_b/\sqrt{2}\sin\beta$. In these rescaled coordinates, we see that the interaction term mixes different two-body angular momentum ℓ sectors.

For low-energies, however, the higher angular momentum channels are subject to a large centrifugal barrier, which allows the interaction terms that mix angular momentum sectors to be treated perturbatively. In particular, for an interaction potential that falls off as $1/r^\delta$ with $\delta > 3$ and for $\ell + \ell' \geq 2$, the scattering-matrix elements (so-called T matrix) scale as [55,56]

$$|T_{\ell\ell'}^{(m)}| \sim \mathrm{const}\, k^{\ell+\ell'+1} + \mathrm{const}\, k^{\delta-2}. \tag{9}$$

We numerically verify these scalings near threshold for a large value of the mass ratio in the Supplemental Material [46]. These scalings suggest that the potential appears completely isotropic near threshold as all the partial waves beyond the s-wave channel ℓ, $\ell' > 0$ are suppressed in the absence of higher-partial wave resonances. To tune near unitarity in this system, we take advantage of shape resonances in the s-wave scattering length a. In Fig. 2(c), we show the positions of the first two scattering resonances as a function of the depth of the potential $\sqrt{mU(0)}r_0$, which can be tuned via Ω or Δ.

These features of the two-body problem have important implications for the three-body problem as well. In particular, this analysis directly implies that the three-body hyperspherical potential $U_3(R)$ will have the universal behavior in the region $r_0 \ll R \ll a$ [1,2]

$$-\frac{\sqrt{3}}{2m}\left[\frac{d^2}{dR^2} + \frac{s_0^2+1/4}{R^2}\right]f_n(R) = E_n f_n(R), \tag{10}$$

where $s_0 = 1.00624\ldots$, R is the three-body hyperradius in the rescaled coordinates [46], and f_n is the hyperradial component of the three-body wave function in hyperspherical coordinates. For distances on the order of r_0 this equation is no longer accurate as the character of the two-body interactions [Eq. (1)] become important. However, in the region, $R \ll r_b$ we can also find the hyperspherical potential analytically because the two-body potential approaches a constant. To better understand the intermediate region $r_b \lesssim R \lesssim r_0$, we have performed numerical calculations [57,58] of $U_3(R)$ that include the coupling to higher-partial waves as a perturbative correction to the two-body s-wave potential [46]. The results are shown in Fig. 3(a) for the first scattering resonance with $m_\perp/m_z = 10$. We see good agreement with the two analytic predictions in the small and large R limits. The presence of the long-range $1/R^2$ potential near unitarity shows that the three-body problem will give rise to an Efimov effect with an infinite series of three-body bound states, with energies ($n = 0, 1, \ldots$)

$$E_n = -\frac{\kappa_*^2}{m} e^{-2\pi n/s_0}, \tag{11}$$

while the presence of the centrifugal barrier near $R \sim r_0$ suggests the scaling for the three-body parameter $\kappa_* \sim 1/r_0$ [50,52,59].

Suppression of three-body loss.—In cold-atom systems, the lifetime of the Efimov states is limited by their decay into deeply bound two-body states. In this Rydberg polariton system, we can avoid such effects by tuning the system near the first scattering resonance in Fig. 2(c), where no deep two-body bound states exist. We can also avoid inelastic two-body loss by going to sufficiently large detunings Δ. However, due to the multicomponent nature of the polariton system and the unconventional dispersion relations, three-body loss processes are still allowed whereby energy and momentum is conserved by scattering the polaritons far away from their initial momentum. As shown in Fig. 3(b), near the inflection point, two such

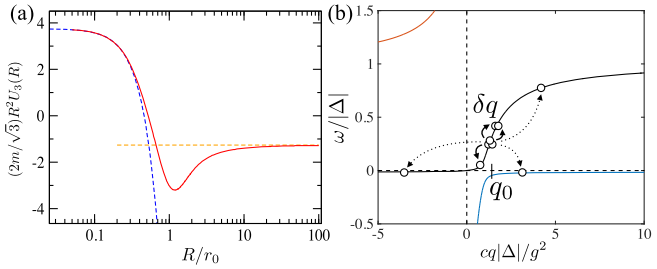

FIG. 3. (a) (red) Rescaled three-body hyperspherical potential at the first scattering resonance for $m_\perp/m_z = 10$. (yellow) In the region $R \gg r_0$, $U_3(R)$ approaches the universal form that gives rise to the Efimov effect. (blue) Analytic result in the region $R \ll r_b$. (b) Three-body loss processes near inflection point (same branch and different branch, see text), where q_0 is the incoming momentum of the polaritons.

three-body loss processes are allowed. In one case, one of the polaritons has a final state on the lower polariton branch, while, in the other case, all three polaritons end on the dark-state branch. On EIT resonance, energy and momentum conservation only allow the former process.

Despite the presence of these additional loss channels, we find that their contribution to the three-body loss is strongly suppressed because the Rydberg blockade mechanism leads to an exponentially small two-body potential for large relative momenta $\delta q \gg r_b^{-1}$. In particular, for the three-body loss channels in Fig. 3(b), each process involves a finite momentum transfer δq. When the minimum $\delta q \gg r_b^{-1}$, we can estimate the three-body loss rate perturbatively in the Fourier transform of $U(r)$, which, it is readily seen, is exponentially suppressed as $e^{-\delta q r_b}$. Near the inflection point, the minimum δq (and thus, the dominant channel) occurs for the process where all three polaritons end on the dark-state branch. By analytically expanding the dispersion to third order around the momentum of the polaritons, we find that the three-body losses will be suppressed when

$$\delta q_z r_b \approx \left(\frac{g^2}{c k_0 \Delta}\right)^{5/3} (r_b k_0)^{1/3} \frac{\Phi^{2/3}}{\beta^3} \gg 1, \tag{12}$$

where the value of $\Phi \equiv \sqrt{mU(0)}r_0$ is determined by the position of the first scattering resonance [e.g., see Fig. 2(c)]. In the Supplemental Material, we provide a more detailed discussion of the scaling of the three-body loss parameter [46]. For a density of 10^{13} cm^{-3} with a blockade radius of 20 μm [27], this implies that β should be less than 0.1 to strongly suppress the three-body losses.

On EIT resonance, the minimum δq for the three-body loss resonance scales as $g^2/c\Delta$. This scaling implies that three-body loss will still play an important role near the first scattering resonance because, on EIT resonance, $\Phi \approx \phi$. Thus, we see the primary advantage of working near the inflection point is the control it provides over the mass ratio, scattering length, and three-body loss rate.

Preparation and detection.—To prepare the Efimov states, we propose using the high-degree of control over the two-body parameters to tune the scattering length ($a < 0$) to values in which the trimers cross zero energy. As each such value is crossed in the space of control parameters, an Efimov state will emerge in transmission through the medium due to the quench dynamics described in the introduction. When more than one Efimov state is present in the medium, they can be distinguished from each other by changing the transverse focus of the input field to increase the initial overlap with the desired state. We give a more detailed discussion of the experimental requirements for realizing long-lived Efimov trimers of Rydberg polaritons in the Supplemental Material [46]. More generally, we remark that the low-energy nature of the Efimov states will render them insensitive to many corrections arising from

short-range physics; thus, we expect their emergence to be a robust feature of the Rydberg polariton system whenever it is possible to tune near a resonance in the 3D two-body scattering length.

Conclusions.—We have demonstrated that systems of interacting photons formed from Rydberg polaritons naturally give rise to an Efimov effect. A potential advantage of this approach is that one can realize long-lived Efimov trimers by tuning near the first scattering resonance and suppressing other three-body loss channels. The wide range of control over the system parameters and the ability to suppress N-body losses make this a promising platform for studying few-body universality. At the same time, increasing the input light intensity provides access to the nonequilibrium, many-body regime where the role of universal few-body physics is poorly understood. The resulting photonic states that emerge from the medium have a rich multiparticle entanglement structure, which may enable them to be used as a resource for optics-based quantum technologies [53,60].

We acknowledge helpful discussions with W. D. Phillips, T. Porto, H. P. Büchler, P. Zoller, M. D. Lukin, V. Vuletic, and Q.-Y. Liang. M. J. G. and S. D. would like to thank the organizers of the workshop on "Quantum Simulation and Many-Body Physics with Light" in Crete, Greece where some of this work was completed. This research was supported by the European Research Council through Grant Agreement No. 647434 (DOQS), NSF through Grant No. PHY-1607204, ARL CDQI, NSF QIS, AFOSR, ARO, ARO MURI, and the NSF-funded Physics Frontier Center at the JQI.

*Present address: Department of Physics, Princeton University, Princeton, NJ 08544, USA.
mgullans@princeton.edu
†gorshkov@umd.edu
‡jmtaylor@jqi.umd.edu

[1] V. N. Efimov, Sov. J. Nucl. Phys. **12**, 589 (1971); Effective interaction of three resonantly interacting particles and the force range, Phys. Rev. C **47**, 1876 (1993).
[2] E. Braaten and H. W. Hammer, Universality in few-body systems with large scattering length, Phys. Rep. **428**, 259 (2006).
[3] T. Kraemer, M. Mark, P. Waldburger, J. G. Danzl, C. Chin, B. Engeser, A. D. Lange, K. Pilch, A. Jaakkola, H. C. Nägerl *et al.*, Evidence for Efimov quantum states in an ultracold gas of caesium atoms, Nature (London) **440**, 315 (2006).
[4] Y. Nishida, Y. Kato, and C. D. Batista, Efimov effect in quantum magnets, Nat. Phys. **9**, 93 (2013).
[5] M. Kunitski, S. Zeller, J. Voigtsberger, A. Kalinin, L. P. H. Schmidt, M. Schoffler, A. Czasch, W. Schollkopf, R. E. Grisenti, T. Jahnke *et al.*, Observation of the Efimov state of the helium trimer, Science **348**, 551 (2015).
[6] L. Platter, H.-W. Hammer, and Ulf-G. Meißner, Four-boson system with short-range interactions, Phys. Rev. A **70**, 052101 (2004).
[7] H. W. Hammer and L. Platter, Universal properties of the four-body system with large scattering length, Eur. Phys. J. A **32**, 113 (2007).
[8] F. Ferlaino, S. Knoop, M. Berninger, W. Harm, J. P. D'Incao, H.-C. Nägerl, and R. Grimm, Evidence for Universal Four-Body States Tied to an Efimov Trimer, Phys. Rev. Lett. **102**, 140401 (2009).
[9] J. von Stecher, J. P. D'Incao, and C. H. Greene, Signatures of universal four-body phenomena and their relation to the Efimov effect, Nat. Phys. **5**, 417 (2009).
[10] N. Mehta, S. Rittenhouse, J. D'Incao, J. von Stecher, and C. Greene, General Theoretical Description of N-Body Recombination, Phys. Rev. Lett. **103**, 153201 (2009).
[11] R. Schmidt and S. Moroz, Renormalization-group study of the four-body problem, Phys. Rev. A **81**, 052709 (2010).
[12] A. Zenesini, B. Huang, M. Berninger, S. Besler, H.-C. Ngerl, F. Ferlaino, R. Grimm, C. H. Greene, and J. von Stecher, Resonant five-body recombination in an ultracold gas of bosonic atoms, New J. Phys. **15**, 043040 (2013).
[13] C. H. Greene, P. Giannakeas, and J. Perez-Rios, Universal few-body physics and cluster formation, Rev. Mod. Phys. **89**, 035006 (2017).
[14] C. E. Klauss, X. Xie, C. Lopez-Abadia, J. P. D'Incao, Z. Hadzibabic, D. S. Jin, and E. A. Cornell, Observation of Efimov Molecules Created from a Resonantly Interacting Bose Gas, Phys. Rev. Lett. **119**, 143401 (2017).
[15] E. Braaten, H. W. Hammer, and M. Kusunoki, Efimov States in a Bose-Einstein Condensate near a Feshbach Resonance, Phys. Rev. Lett. **90**, 170402 (2003).
[16] J. D. Pritchard, D. Maxwell, A. Gauguet, K. J. Weatherill, M. P. A. Jones, and C. S. Adams, Cooperative Atom-Light Interaction in a Blockaded Rydberg Ensemble, Phys. Rev. Lett. **105**, 193603 (2010).
[17] A. V. Gorshkov, J. Otterbach, M. Fleischhauer, T. Pohl, and M. D. Lukin, Photon-Photon Interactions via Rydberg Blockade, Phys. Rev. Lett. **107**, 133602 (2011).
[18] Y. O. Dudin and A. Kuzmich, Strongly interacting Rydberg excitations of a cold atomic gas, Science **336**, 887 (2012).
[19] T. Peyronel, O. Firstenberg, Q.-Y. Liang, S. Hofferberth, A. V. Gorshkov, T. Pohl, M. D. Lukin, and V. Vuletic, Quantum nonlinear optics with single photons enabled by strongly interacting atoms, Nature (London) **488**, 57 (2012).
[20] H. Gorniaczyk, C. Tresp, J. Schmidt, H. Fedder, and S. Hofferberth, Single-Photon Transistor Mediated by Interstate Rydberg Interactions, Phys. Rev. Lett. **113**, 053601 (2014).
[21] D. Tiarks, S. Baur, K. Schneider, S. Dürr, and G. Rempe, Single-Photon Transistor Using a Förster Resonance, Phys. Rev. Lett. **113**, 053602 (2014).
[22] S. Baur, D. Tiarks, G. Rempe, and S. Dürr, Single-Photon Switch Based on Rydberg Blockade, Phys. Rev. Lett. **112**, 073901 (2014).
[23] D. Tiarks, S. Schmidt, G. Rempe, and S. Dürr, Optical π phase shift created with a single-photon pulse, Sci. Adv. **2**, e1600036 (2016).
[24] J. D. Thompson, T. L. Nicholson, Q.-Y. Liang, S. H. Cantu, A. V. Venkatramani, S. Choi, I. A. Fedorov, D. Viscor, T. Pohl, M. D. Lukin *et al.*, Symmetry-protected collisions between strongly interacting photons, Nature (London) **542**, 206 (2017).

[25] C. R. Murray and T. Pohl, Coherent Photon Manipulation in Interacting Atomic Ensembles, Phys. Rev. X **7**, 031007 (2017).
[26] H. Busche, P. Huillery, S. W. Ball, T. Ilieva, M. P. A. Jones, and C. S. Adams, Contactless nonlinear optics mediated by long-range Rydberg interactions, Nat. Phys. **13**, 655 (2017).
[27] O. Firstenberg, T. Peyronel, Q.-Y. Liang, A. V. Gorshkov, M. D. Lukin, and V. Vuletić, Attractive photons in a quantum nonlinear medium, Nature (London) **502**, 71 (2013).
[28] P. Bienias, S. Choi, O. Firstenberg, M. F. Maghrebi, M. Gullans, M. D. Lukin, A. V. Gorshkov, and H. P. Büchler, Scattering resonances and bound states for strongly interacting Rydberg polaritons, Phys. Rev. A **90**, 053804 (2014).
[29] M. F. Maghrebi, M. J. Gullans, P. Bienias, S. Choi, I. Martin, O. Firstenberg, M. D. Lukin, H. P. Büchler, and A. V. Gorshkov, Coulomb Bound States of Strongly Interacting Photons, Phys. Rev. Lett. **115**, 123601 (2015).
[30] M. J. Gullans, J. D. Thompson, Y. Wang, Q.-Y. Liang, V. Vuletić, M. D. Lukin, and A. V. Gorshkov, Effective Field Theory for Rydberg Polaritons, Phys. Rev. Lett. **117**, 113601 (2016).
[31] K. Jachymski, P. Bienias, and H. P. Büchler, Three-Body Interaction of Rydberg Slow-Light Polaritons, Phys. Rev. Lett. **117**, 053601 (2016).
[32] Q.-Y. Liang, A. V. Venkatramani, S. H. Cantu, T. L. Nicholson, M. J. Gullans, A. V. Gorshkov, J. D. Thompson, C. Chin, M. D. Lukin, and V. Vuletić, Observation of three-photon bound states in a quantum nonlinear medium, arXiv:1709.01478.
[33] M. J. Gullans *et al.* (to be published).
[34] T. Pohl, E. Demler, and M. D. Lukin, Dynamical Crystallization in the Dipole Blockade of Ultracold Atoms, Phys. Rev. Lett. **104**, 043002 (2010).
[35] V. Parigi, E. Bimbard, J. Stanojevic, A. J. Hilliard, F. Nogrette, R. Tualle-Brouri, A. Ourjoumtsev, and P. Grangier, Observation and Measurement of Interaction-Induced Dispersive Optical Nonlinearities in an Ensemble of Cold Rydberg Atoms, Phys. Rev. Lett. **109**, 233602 (2012).
[36] J. Otterbach, M. Moos, D. Muth, and M. Fleischhauer, Wigner Crystallization of Single Photons in Cold Rydberg Ensembles, Phys. Rev. Lett. **111**, 113001 (2013).
[37] A. V. Gorshkov, R. Nath, and T. Pohl, Dissipative Many-Body Quantum Optics in Rydberg Media, Phys. Rev. Lett. **110**, 153601 (2013).
[38] M. F. Maghrebi, N. Y. Yao, M. Hafezi, T. Pohl, O. Firstenberg, and A. V. Gorshkov, Fractional quantum Hall states of Rydberg polaritons, Phys. Rev. A **91**, 033838 (2015).
[39] M. Moos, M. Höning, R. Unanyan, and M. Fleischhauer, Many-body physics of Rydberg dark-state polaritons in the strongly interacting regime, Phys. Rev. A **92**, 053846 (2015).
[40] A. Sommer, H. P. Büchler, and J. Simon, Quantum crystals and Laughlin droplets of cavity Rydberg polaritons, arXiv:1506.00341.
[41] A. Grankin, E. Brion, R. Boddeda, S. Ćuk, I. Usmani, A. Ourjoumtsev, and P. Grangier, Inelastic Photon Scattering via the Intracavity Rydberg Blockade, Phys. Rev. Lett. **117**, 253602 (2016).
[42] N. Schine, A. Ryou, A. Gromov, A. Sommer, and J. Simon, Synthetic Landau levels for photons, Nature (London) **534**, 671 (2016).
[43] N. Jia, N. Schine, A. Georgakopoulos, A. Ryou, A. Sommer, and J. Simon, A strongly interacting polaritonic quantum dot, arXiv:1705.07475.
[44] E. Zeuthen, M. J. Gullans, M. F. Maghrebi, and A. V. Gorshkov, Correlated Photon Dynamics in Dissipative Rydberg Media, Phys. Rev. Lett. **119**, 043602 (2017).
[45] M. D. Lukin, M. Fleischhauer, R. Cote, L. M. Duan, D. Jaksch, J. I. Cirac, and P. Zoller, Dipole Blockade and Quantum Information Processing in Mesoscopic Atomic Ensembles, Phys. Rev. Lett. **87**, 037901 (2001).
[46] See Supplemental Material at http://link.aps.org/supplemental/10.1103/PhysRevLett.119.233601 for more details on two-body scattering with anisotropic mass, scaling analysis of three-body loss rate, perturbative treatment of the anisotropic mass, and further discussion of experimental requirements, which includes Refs. [47–49].
[47] E. Braaten and H. W. Hammer, Three-Body Recombination into Deep Bound States in a Bose Gas with Large Scattering Length, Phys. Rev. Lett. **87**, 160407 (2001).
[48] J. B. Balewski, A. T. Krupp, A. Gaj, D. Peter, H. P. Büchler, R. Löw, S. Hofferberth, and T. Pfau, Coupling a single electron to a Bose-Einstein condensate, Nature (London) **502**, 664 (2013).
[49] A. Derevianko, P. Kómár, T. Topcu, R. M. Kroeze, and M. D. Lukin, Effects of molecular resonances on Rydberg blockade, Phys. Rev. A **92**, 063419 (2015).
[50] J. Wang, J. P. D'Incao, B. D. Esry, and C. H. Greene, Origin of the Three-Body Parameter Universality in Efimov Physics, Phys. Rev. Lett. **108**, 263001 (2012).
[51] P. Naidon, S. Endo, and M. Ueda, Physical origin of the universal three-body parameter in atomic Efimov physics, Phys. Rev. A **90**, 022106 (2014).
[52] P. Naidon, S. Endo, and M. Ueda, Microscopic Origin and Universality Classes of the Efimov Three-Body Parameter, Phys. Rev. Lett. **112**, 105301 (2014).
[53] J.-W. Pan, Z.-B. Chen, C.-Y. Lu, H. Weinfurter, A. Zeilinger, and M. Żukowski, Multiphoton entanglement and interferometry, Rev. Mod. Phys. **84**, 777 (2012).
[54] R. H. Dicke, Coherence in spontaneous radiation processes, Phys. Rev. **93**, 99 (1954).
[55] H. R. Sadeghpour, J. L. Bohn, M. J. Cavagnero, B. D. Esry, I. I. Fabrikant, J. H. Macek, and A. R. P. Rau, Collisions near threshold in atomic and molecular physics, J. Phys. B **33**, R93 (2000).
[56] J. L. Bohn, M. Cavagnero, and C. Ticknor, Quasi-universal dipolar scattering in cold and ultracold gases, New J. Phys. **11**, 055039 (2009).
[57] J. P. D'Incao and B. D. Esry, Manifestations of the Efimov effect for three identical bosons, Phys. Rev. A **72**, 032710 (2005).
[58] J. Wang, J. P. D'Incao, and C. H. Greene, Numerical study of three-body recombination for systems with many bound states, Phys. Rev. A **84**, 052721 (2011).
[59] Y. Wang, J. P. D'Incao, and C. H. Greene, Efimov Effect for Three Interacting Bosonic Dipoles, Phys. Rev. Lett. **106**, 233201 (2011).
[60] L. K. Shalm, D. R. Hamel, Z. Yan, C. Simon, K. J. Resch, and T. Jennewein, Three-photon energy–time entanglement, Nat. Phys. **9**, 19 (2013).